ISSN 2250-3153

Climate Predictions of the Twenty First Century Based on Skill Selected Global Climate Models

J. Masanganise, T.W. Mapuwei, M. Magodora, C. Shonhiwa

Department of Physics and Mathematics, Bindura University of Science Education, P Bag 1020, Bindura, Zimbabwe

Abstract- A subset of global climate models from the Coupled Model Inter-comparison Project 5 was used to explore the changes in temperature and rainfall under moderate and high climate change scenarios. We used downscaled model projections of daily minimum and maximum temperature and rainfall for the period 2040-2070 relative to the 1980-2010 reference period. Analysis of variance (ANOVA) was used to test (at 5 % level of significance) for differences among the three selected models in predicting the three variables under both climate change scenarios. Where significant differences were observed, we carried out multiple pair-wise comparison of the models using Dunnett's test. Overall, two of the three models showed insignificant differences ($p<0.05$) in predicting minimum and maximum temperature while the other model deviated from the two. However, we identified a consistent warming trend across all the three models. The strength of global climate models in rainfall prediction was found to lie in their ability to simulate extremes, making the models relevant to sectors of the economy that are vulnerable to extreme rainfall such as drought and floods.

Index Terms- downscaled model projections, multiple pair-wise comparison, extreme rainfall.

I. INTRODUCTION

A variety of processes characterise the climate system. Some of them include; boundary layer processes, radiative processes and cloud processes. These processes interact with each other both spatially and temporarily. Global climate models (GCMs) have been shown to be useful tools for studying the climate system (Pitman and Perkins, 2008; Houghton *et al*., 2001; Randall *et al*., 2007), however because they have limited resolutions at smaller scales, many climate processes are not resolved adequately by climate models. Climate projections of the future remain a challenge to many climate modeling communities. Chiew *et al*. (2009) point out that climate change impact assessment is likely to be more reliable if it is based on future climate projections from the better GCMs. However, it is difficult to objectively determine which GCMs are more likely to give reliable future climate projections. Pitman and Perkins (Pitman and Perkins, 2008) carried out climate projections for Australia using GCMs. The authors based their study on the assumption that a model that is able to simulate the probability density function (PDF) of a climate variable well for the twentieth century is likely to be able to simulate well the future PDF of the same variable. Pitman and Perkins (2008) reported a considerable overlap between the PDFs of the twentieth century and those of the twenty first century. In this paper, we attempt to provide climate projections of the twenty first century in Zimbabwe, based on skill selected global climate models from the Coupled Model Inter-comparison Project 5 (CMIP5). The GCMs are based on the recently developed Representative Concentration Pathway (RCP) emission scenarios. Measures of model skill have been presented using a variety of metrics (e.g. Johnson and Sharma, 2009; Carmen Sa´nchez de Cos, 2012; Boberg *et al*., 2009; Perkins *et al*., 2007; Masanganise *et al*., 2013). We follow the methodology of Masanganise *et al*. (2014a) to select models that are highly skilful at simulating daily probability density functions of maximum temperature (T_{max}), minimum temperature (T_{min}) and rainfall (R). Masanganise *et al*. (2014a) used probability density functions to compare daily model simulations with daily observed climatology over the same period. To rank the models, the authors used a match metric method based on the common overlap of the model and observed PDFs with a skill score value ranging from zero for no overlap to a skill score of one for a perfect overlap. Using this method, we select three models that best match observations for each variable out of ten models and apply them to make climate projections of the mid-century (2040-2070) period relative to the 1980-2010 baseline period. The projections are based on the moderate (RCP4.5) emission scenario and the highest (RCP8.5) emission scenario. The methodology is provided in section 2, results and discussion in section 3 and lastly, conclusions in section 4.

II. DATA AND METHODOLOGY

The study was carried out in Zimbabwe in a district called Mutoko. The climatic variables used were maximum air temperature T_{max}, minimum air temperature T_{min} and rainfall R. The choice of these three variables was partly based on data availability. Details of data acquisition and processing are presented in Masanganise *et al*. (2014a). The GCMs used are listed in Table l.

Table 1 A list of the 10 coupled global climate models from which 3 models were selected.

Model name	Modeling centre(or group)	Resolution (degrees) latitude x longitude
Beijing Normal University Earth System model (BNU-ESM)	College of Global Change and Earth System Science, Beijing Normal University, China	2.810 x 2.810
Canadian Earth System Model version 2 (CanESM2)	Canadian Centre for Climate Modelling and Analysis, Canada	2.810 x 2.810
Centre National de Recherche Météorologiques Climate Model version 5 (CNRM-CM5)	CNRM/Centre Europeen de Recherche et Formation Avancees en Calcul Scientifique, France Calcul Scientifique, France	1.410 x 1.410
Flexible Global Ocean-Atmosphere-Land System Modelspectral version 2 (FGOALS-s2)	State Key Laboratory of Numerical Modeling for Atmospheric Sciences and Geophysical Fluid Dynamics, Institute of Atmospheric Physics, Chinese Academy of Sciences, China	1.670 x 2.810
Geophysical Fluid Dynamics Laboratory Earth System Model (GFDL-ESM2G)	NOAA Geophysical Fluid Dynamics Laboratory	2.000 x 2.500
Geophysical Fluid Dynamics Laboratory Earth System Model (GFDL-ESM2M)	NOAA Geophysical Fluid Dynamics Laboratory	2.000 x 2.500
Model for Interdisciplinary Research on Climate-Earth System, version 5 (MIROC5)	The University of Tokyo, National Institute for Environmental Studies and Japan Agency for Marine-Earth Science and Technology	1.417 x 1.406
Atmospheric Chemistry Coupled Version of Model for Interdisciplinary Research on Climate-Earth System (MIROC-ESM-CHEM)	Japan Agency for Marine-Earth Science and Technology, The University of Tokyo and National Institute for Environmental Studies	2.857 x 2.813
Model for Interdisciplinary Research on Climate-Earth System (MIROC-ESM)	Japan Agency for Marine–Earth Science and Technology, The University of Tokyo and National Institute for Environmental Studies	2.857 x 2.813
Meteorological Research Institute Coupled General Circulation Model version 3 (MRI-CGCM3)	Meteorological Research Institute, Japan	1.132 x 1.125

Three models were selected from Table 1 using the match metric method described in Masanganise *et al*. (2014a). For temperature, these were models that were able to capture at least 97 % of the observed probability density function in their simulations. In the case of rainfall, the skill scores were low and we selected only those models that were able to capture at least 31 % of the observed probability density function. We then analysed climate projections for the period 2040-2070 relative to the 1980-2010 baseline based on the three global climate models selected from Table 1.

i. Temperature and rainfall projections

Using downscaled historical (1980-2010) daily data, we calculated monthly mean values for T_{max}, T_{min} and R for each climate change scenario. We also calculated monthly mean values for the same variables and scenarios using projections for the period 2040-2070. Anomalies were then calculated as the absolute difference (2040-2070) minus (1980-2010) for each model and variable to depict the magnitude of change.

ii. Model convergence

Model convergence was assessed using probability density functions (PDFs) to establish the consistency in predictions from the 3 models. We calculated PDFs for each of the variables T_{max}, T_{min} and R using downscaled GCM projections for the period 2040-2070 under RCP4.5 and RCP8.5. The PDFs were constructed using the method described in Masanganise *et al*. (2014a). Analysis of variance (ANOVA) was used to test (at 5 % level of significance) for differences among the three selected models in predicting T_{max}, T_{min} and R under both climate change scenarios. If the differences were observed to be significant under ANOVA, we proceeded to carry out multiple pair-wise comparison of the models using Dunnett's test.

III. Results and Discussion

i. Projections of temperature

Monthly time series plots of temperature anomalies are shown in Figure 3.1 to Figure 3.4

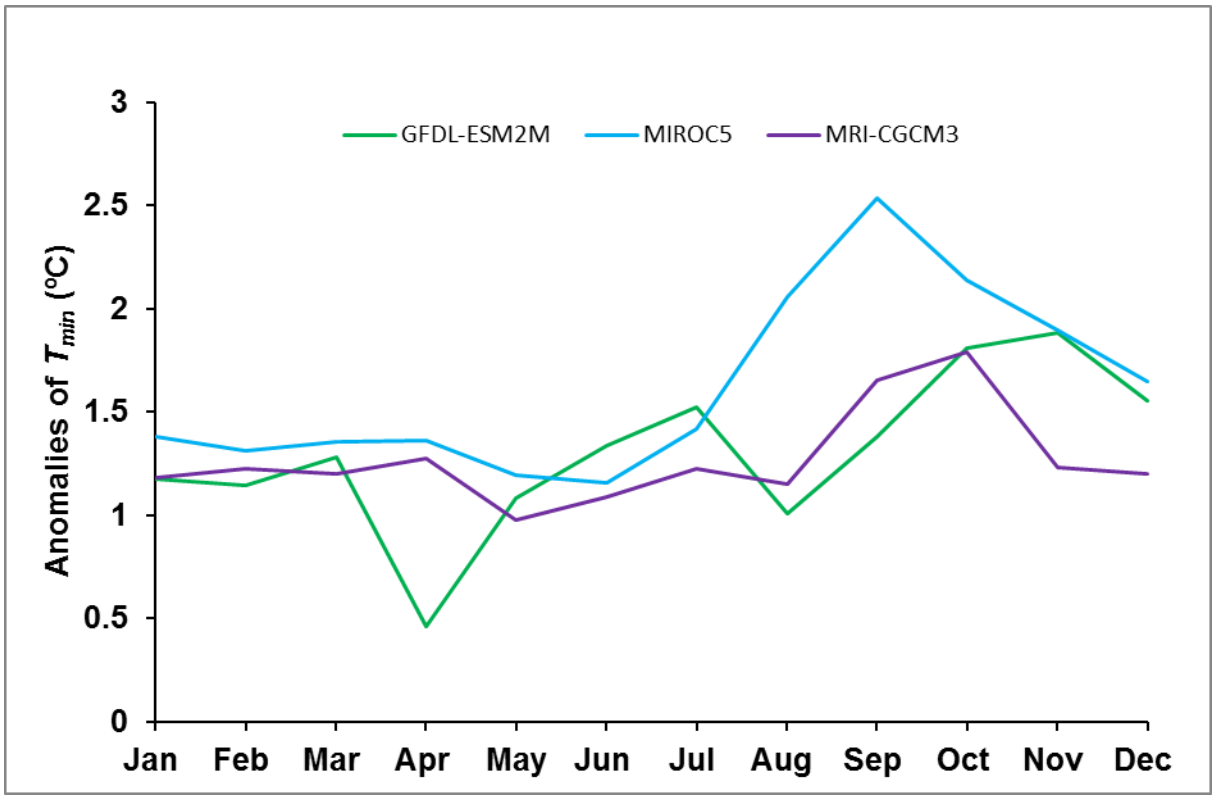

Figure 3.1 Projections of mean monthly anomalies for T_{min} for the period 2040-2070 under RCP4.5

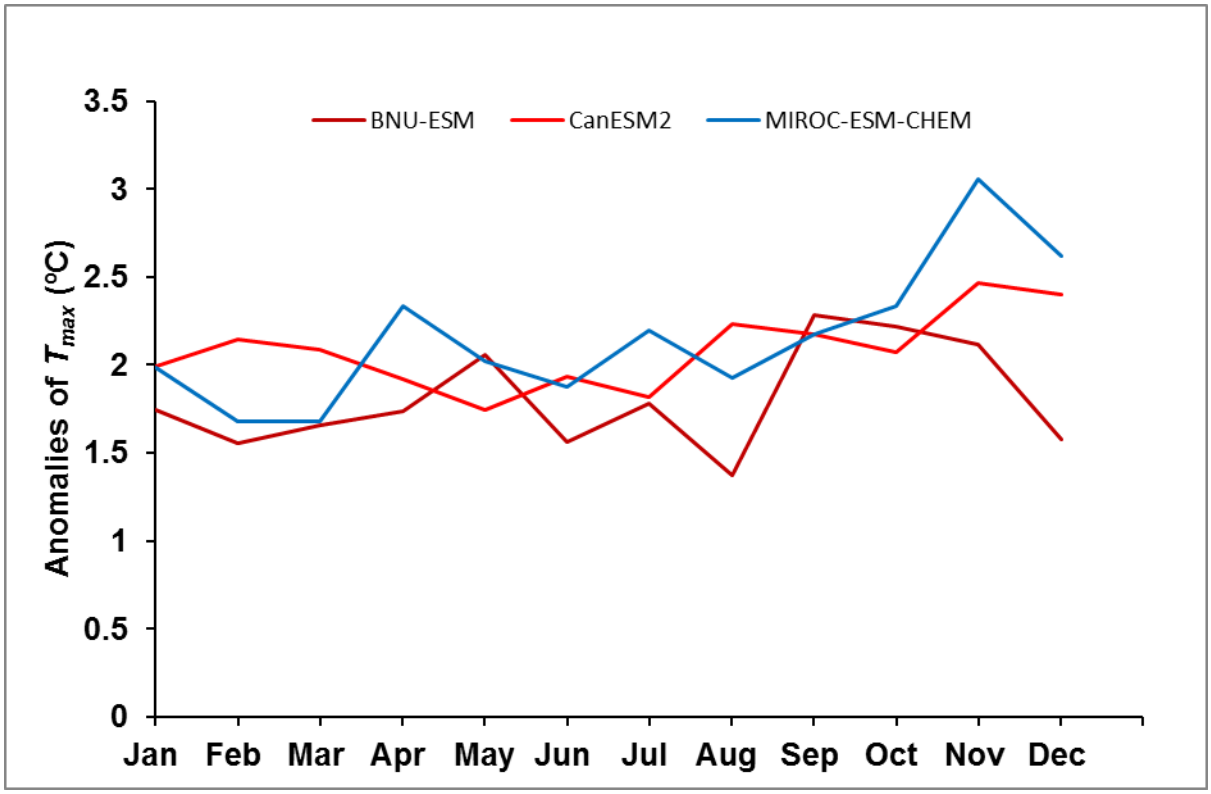

Figure 3.2 Projections of mean monthly anomalies for T_{max} for the period 2040-2070 under RCP4.5

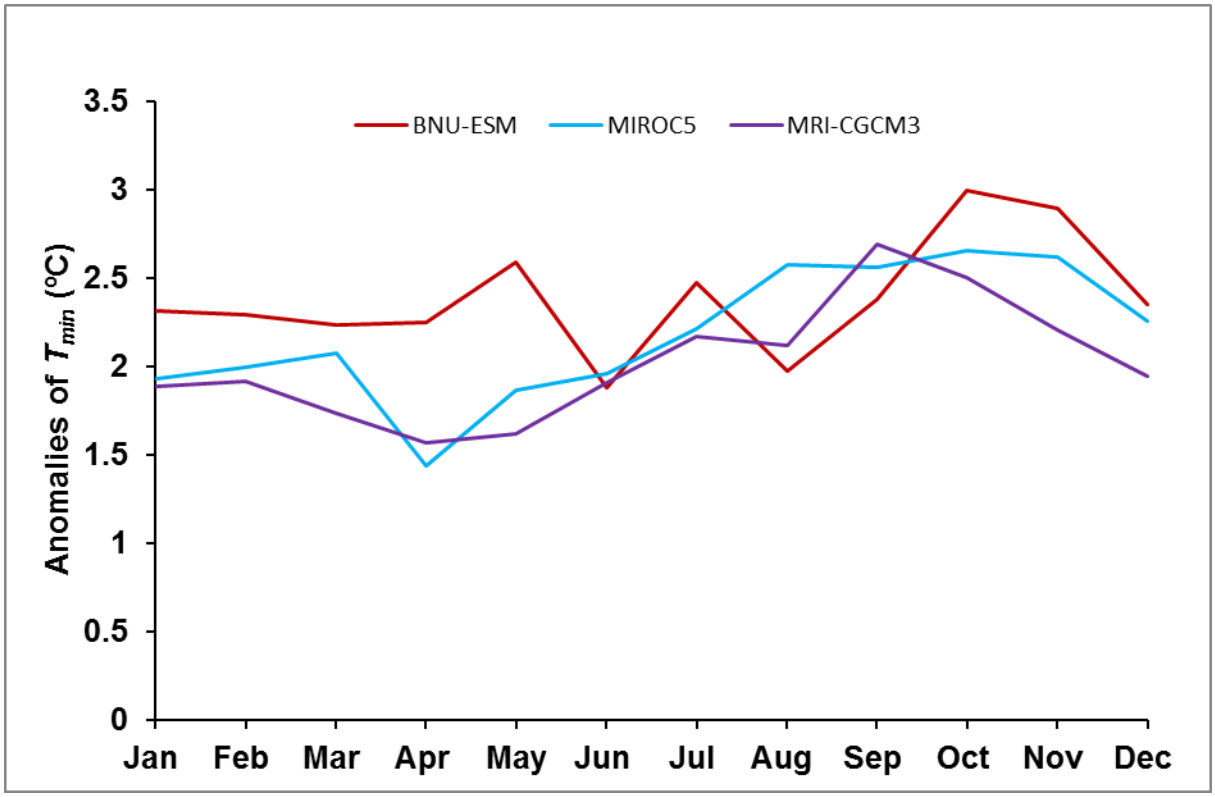

Figure 3.3 Projections of mean monthly anomalies for T_{min} for the period 2040-2070 under RCP8.5

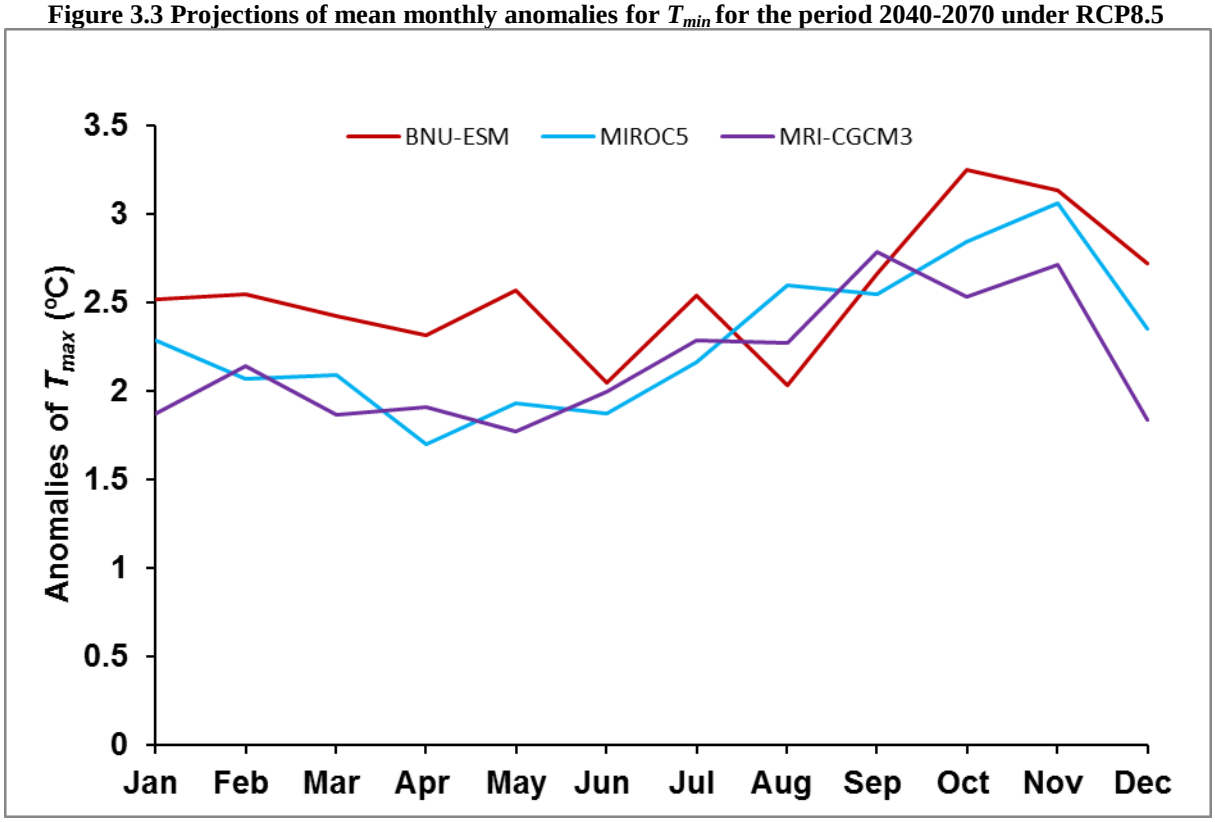

Figure 3.4 Projections of mean monthly anomalies for T_{max} for the period 2040-2070 under RCP8.5

The best three models selected for simulating T_{min} under RCP4.5 were MRI-CGCM3, MIROC5 and GFDL-ESM2M. Figure 3.1 shows the mean monthly temperature changes projected by each model. The three models projected an increase in temperature in the period 2040-2070 above the 1980-2010 baseline. The models were consistent in their projections although the GFDL-ESM2M model deviated from the other two in the month of April while the MIROC5 model showed large deviations in the months of July to October. The best three models selected for simulating T_{max} under

RCP4.5 were CanESM2, BNU-ESM and MIROC-ESM-CHEM. Temperature projections by these models are less than about 1 °C in most of the months as shown in Figure 3.2. Under RCP8.5, the models selected for simulating T_{min} were MRI-CGCM3, MIROC5 and BNU-ESM. The same models were also selected for simulating T_{max}. These models projected a consistent warming trend of about 1 °C or less as shown in Figure 3.3 and Figure 3.4. Time series plots of Figure 3.3 and Figure 3.4 indicate very similar trends predicted by the MRI-CGCM3 and MIROC5 models. By using fewer models, we found a reduction in the amplitude of warming compared to that reported in Masanganise *et al*. (2014b) who applied all the 10 climate models to make climate projections over the same period.

ii. Projections of rainfall

Monthly time series plots of rainfall anomalies are shown in Figure 3.5 and Figure 3.6

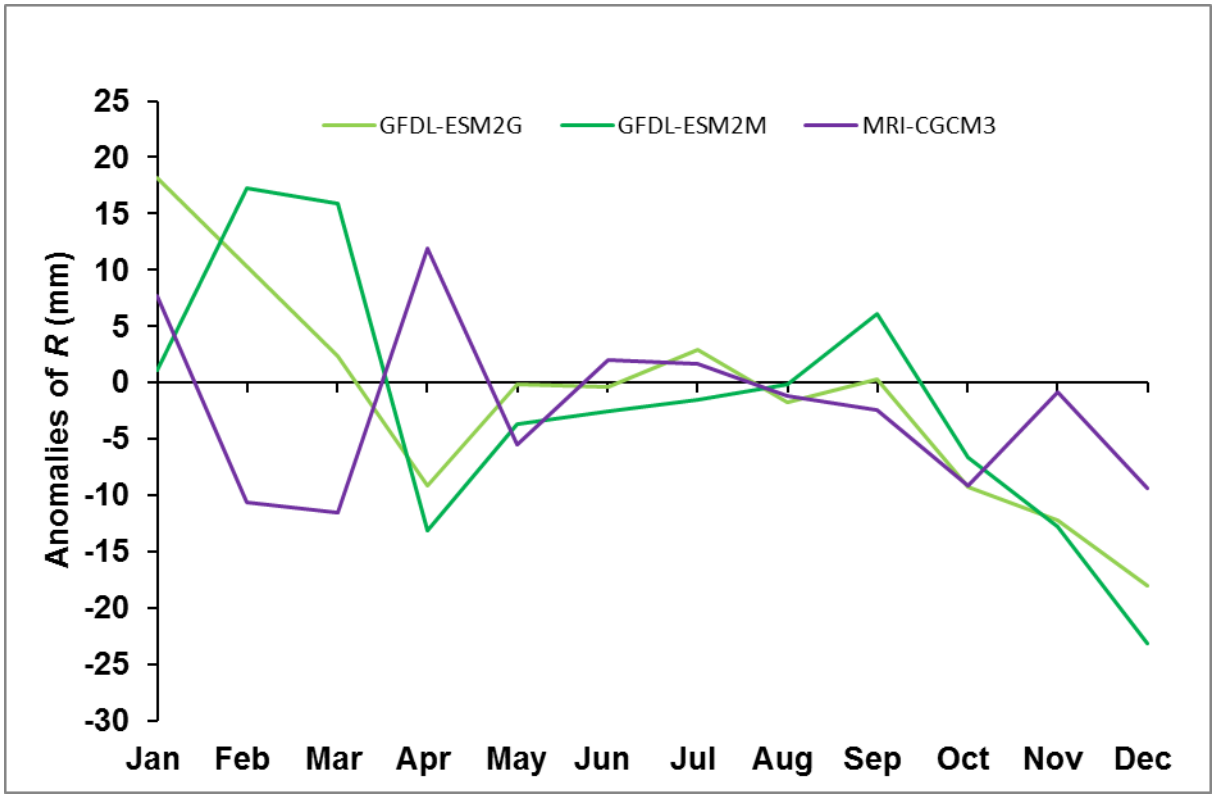

Figure 3.5 Projections of mean monthly anomalies for *R* for the period 2040-2070 under RCP4.5

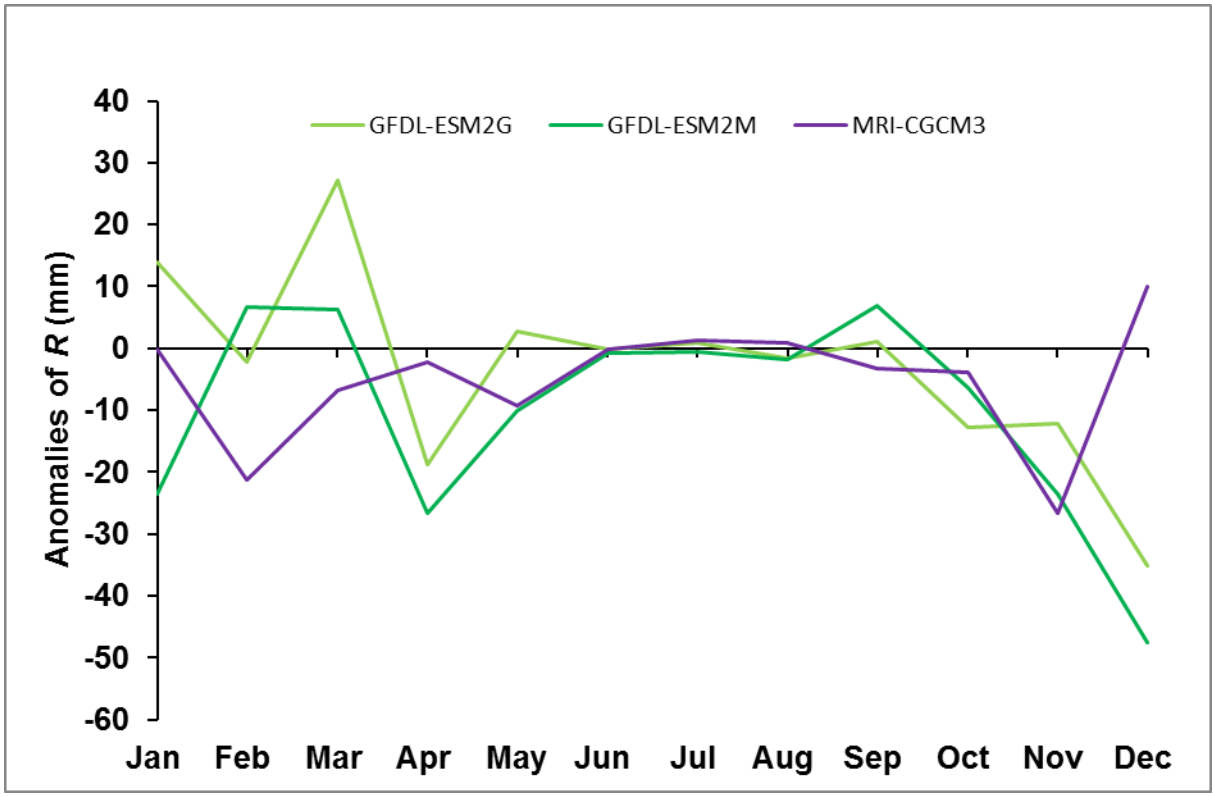

Figure 3.6 Projections of mean monthly anomalies for *R* for the period 2040-2070 under RCP8.5

The best three models selected for simulating *R* under RCP4.5 were GFDL-ESM2G, GFDL-ESM2M and MRI-CGCM3. The same models were also selected for simulating *R* under RCP8.5. Figure 3.5 and Figure 3.6 show the mean monthly rainfall change projections by the three models. There was a wide variation in the predictions by the three models mainly in the months of January-April where the spread of rainfall change projections is large. However, the three models agreed in the direction of rainfall change in the months of October-December under both climate change scenarios supporting findings by Masanganise *et al.* (2014b)

iii. **Analysis of PDFs for T_{min} and T_{max}**

PDFs are shown in Figure 3.7 to Figure 3.10

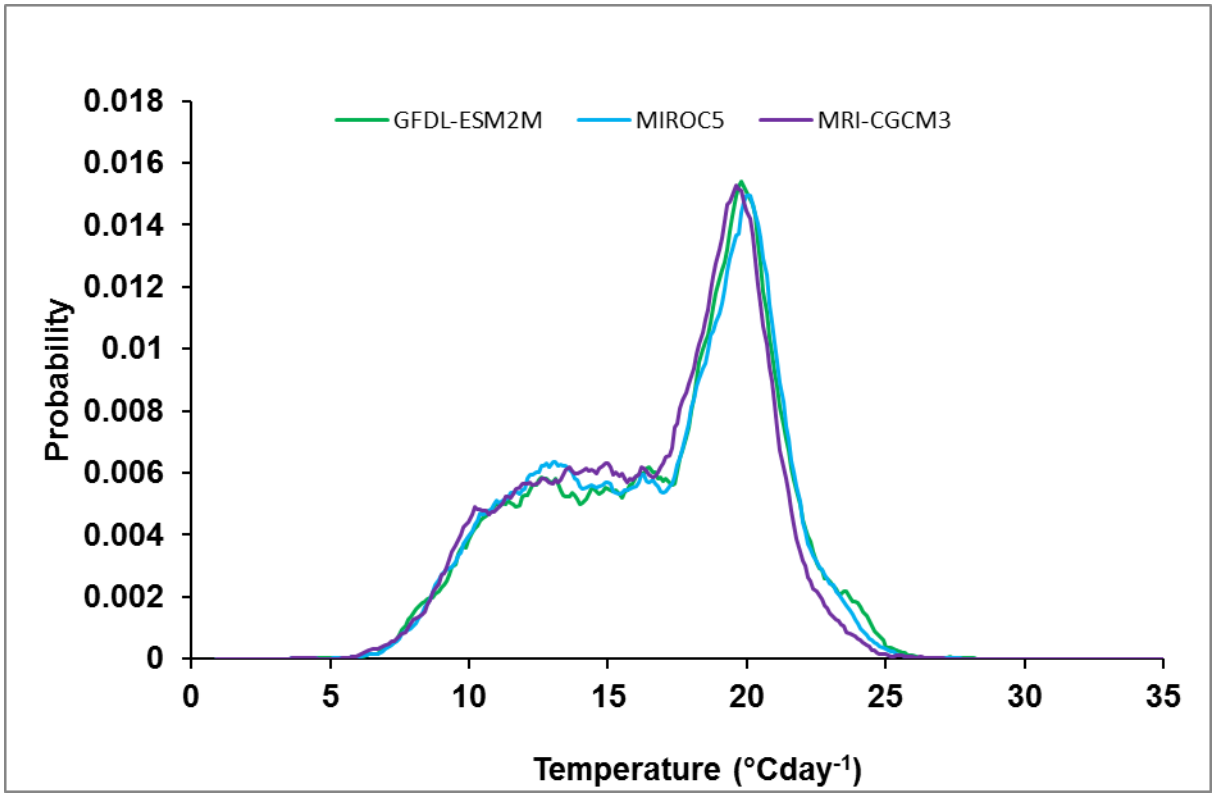

Figure 3.7 Probability density functions of the three models for T_{min} for the period 2040-2070 under RCP4.5

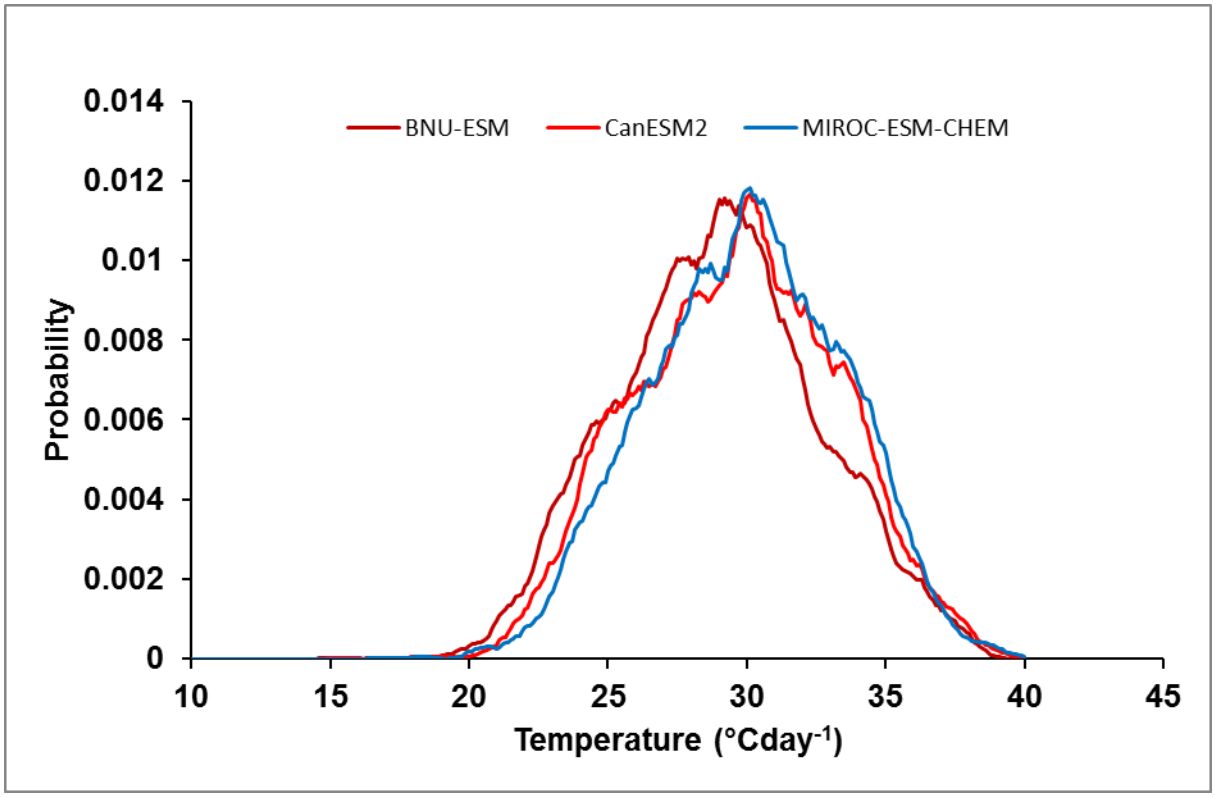

Figure 3.8 Probability density functions of the three models for T_{max} for the period 2040-2070 under RCP4.5

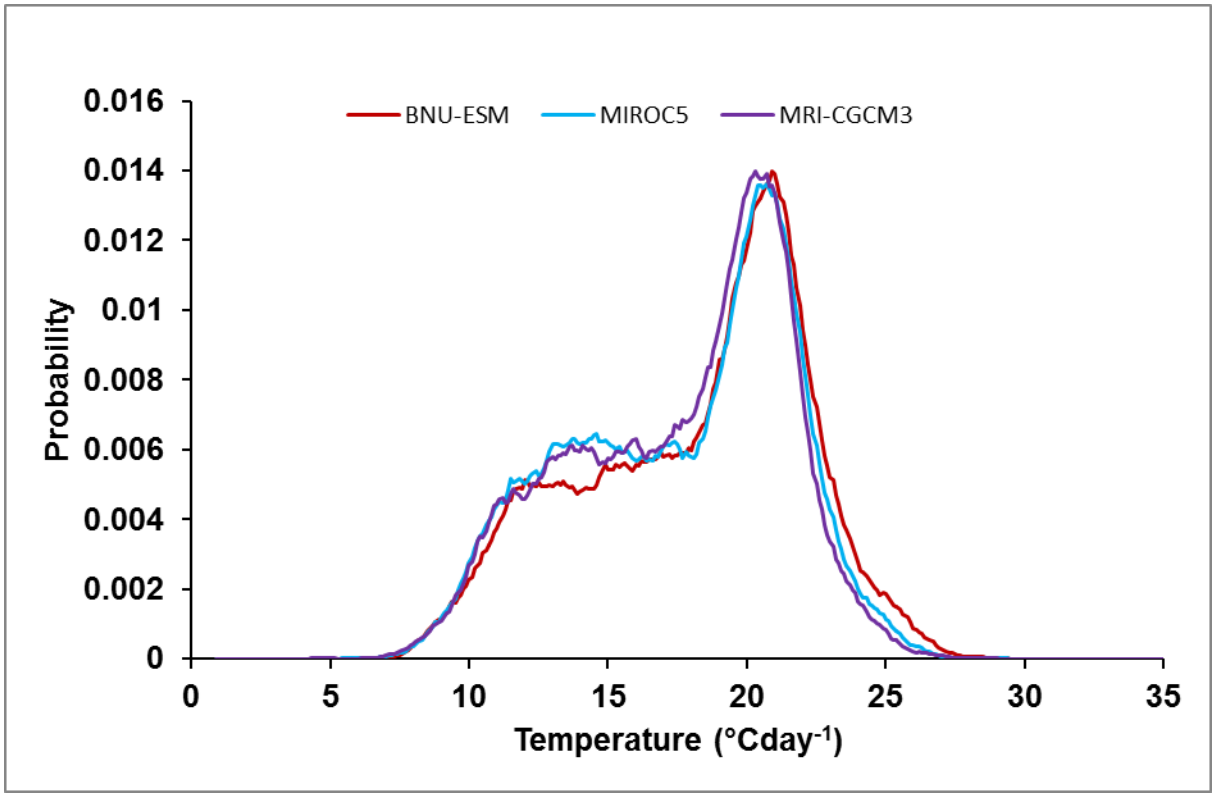

Figure 3.9 Probability density functions of the three models for T_{min} for the period 2040-2070 under RCP8.5

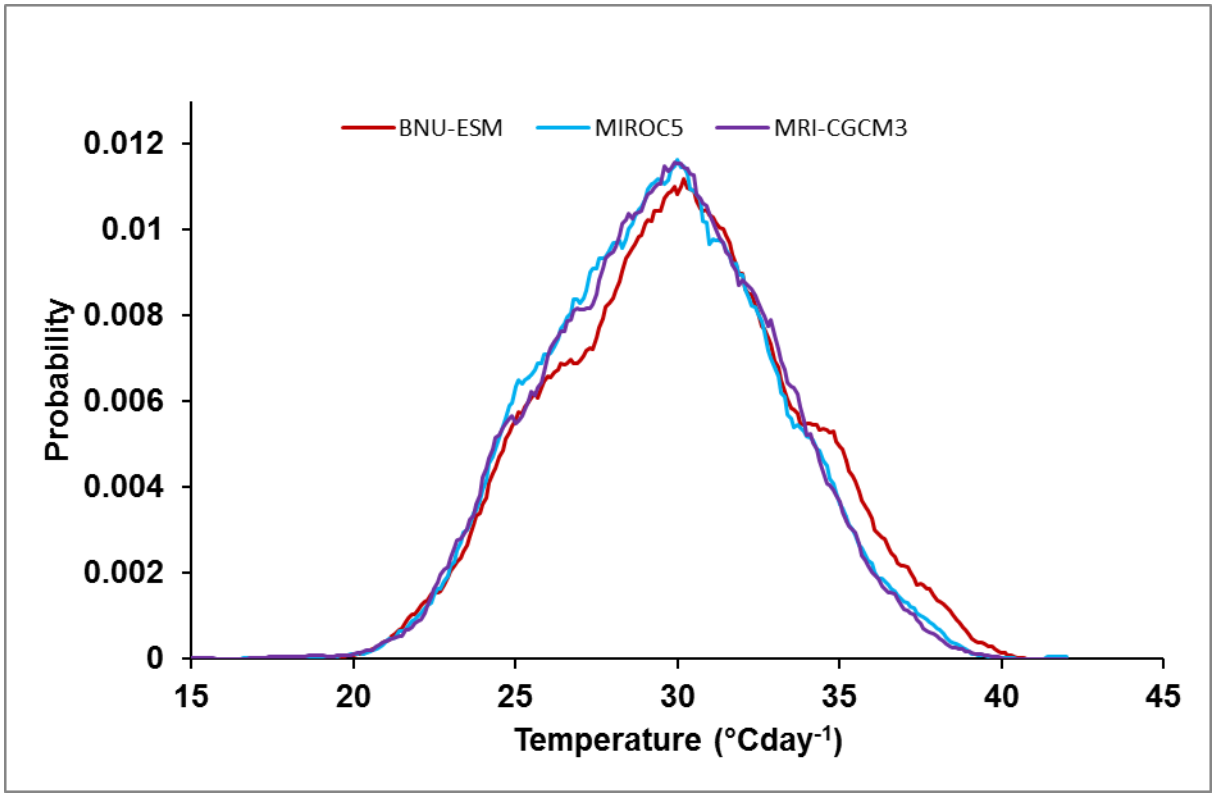

Figure 3.10 Probability density functions of the three models for T_{max} for the period 2040-2070 under RCP8.5

Figure 3.7 to Figure 3.10 show the PDFs for T_{min} and T_{max} for each climate change scenario. Overall, the shapes of the PDFs are in agreement with each other, an indication that the 3 models predicted similar trends. In Figure 3.9 and Figure 3.10, PDFs for the MIROC5 and MRI-CGCM3 are

almost overlapping. This is in agreement with time series plots in Figure 3.3 and Figure 3.4. In general, there was an increase in the amount of overlap of the PDFs when three best models were used as compared to the amount of overlap reported in Masanganise *et al*. (2014b) in which all the 10 models were used.

iv. Analysis of PDFs for *R*

PDFs are shown in Figure 3.11 and Figure 3.12

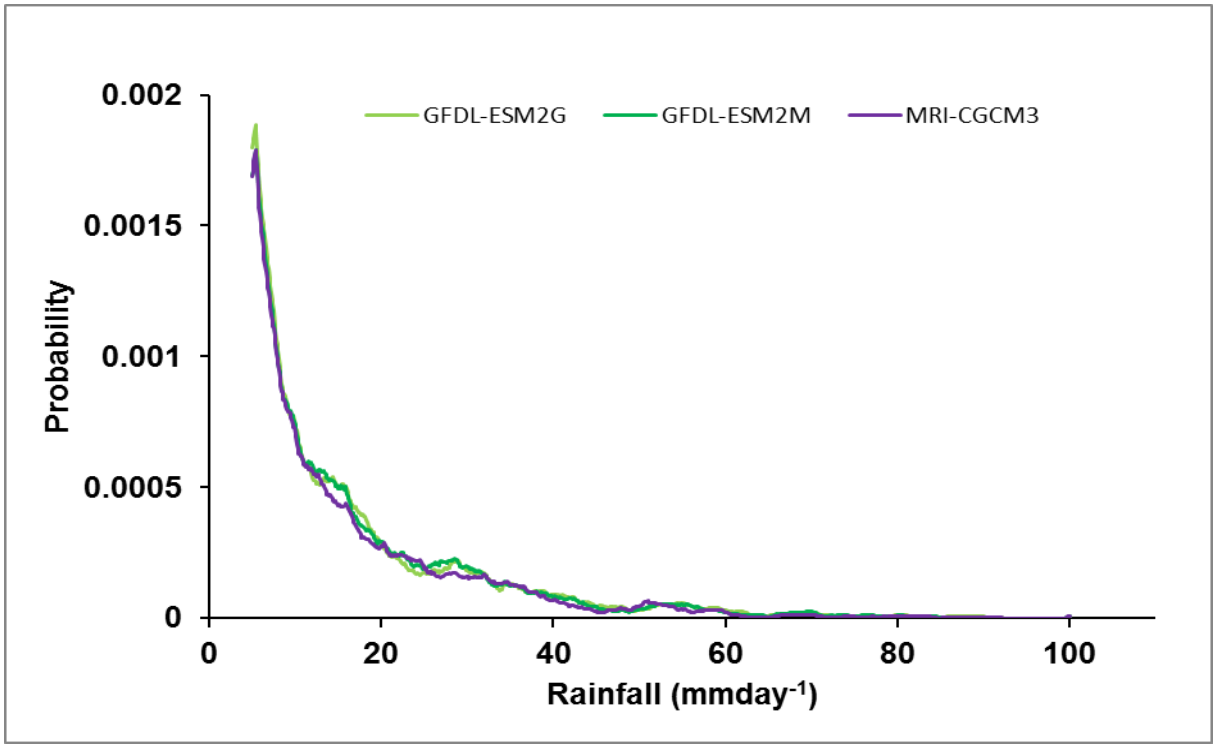

Figure 3.11 Probability density functions of the three models for *R* for the period 2040-2070 under RCP4.5

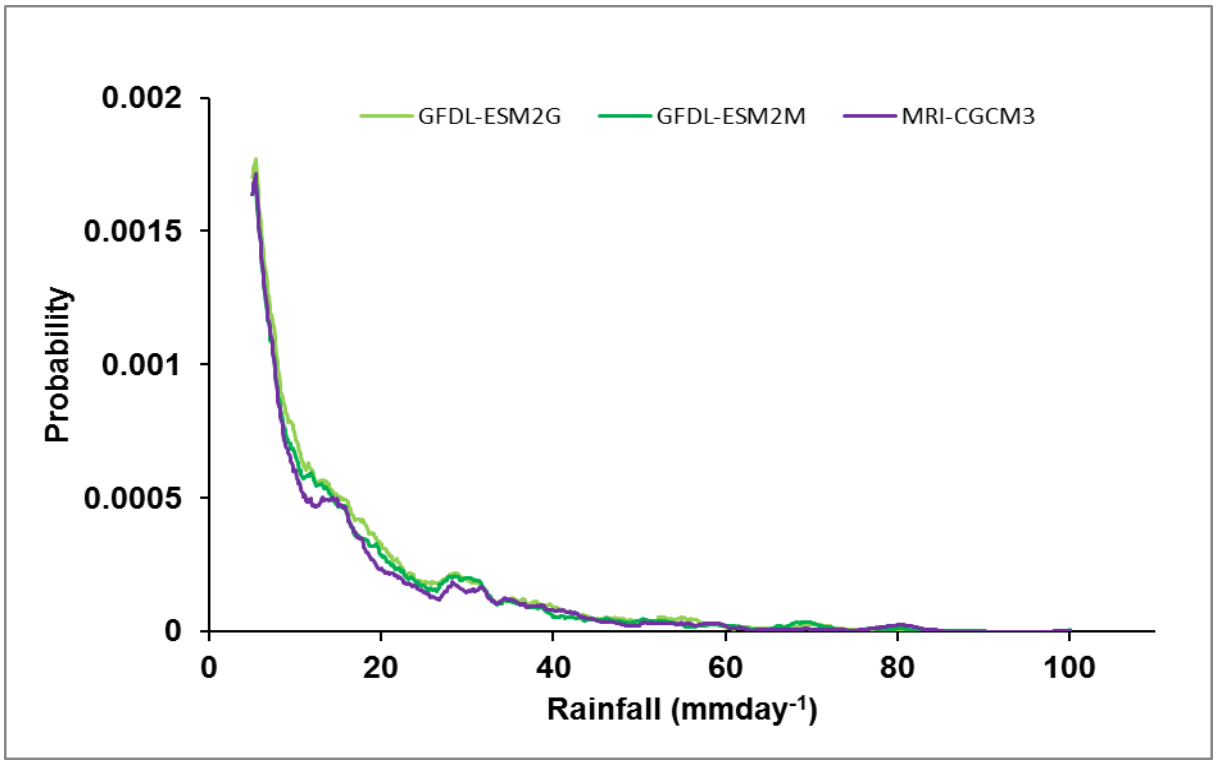

Figure 3.12 Probability density functions of the three models for *R* for the period 2040-2070 under RCP8.5

Figure 3.11 and Figure 3.12 show the PDFs for *R* for the two climate change scenarios. Models tend to agree at the extremes of the distribution as shown by the PDFs clustering in these regions. In between the extremes, PDFs are widely separated indicating some level of disagreement in predictions. Rainfall is difficult to predict than temperature (Pitman and Perkins, 2008) and it is expected that there would be considerable uncertainty in the projections of rainfall using climate models.

v. Analysis of variance (ANOVA) and multiple pair wise comparison.

Table 2 Analysis of variance for predicting T_{min} under RCP4.5

	Sum of Squares	df	Mean Square	F	Sig.
Between Groups	899.278	2	449.639	28.354	.000
Within Groups	538634.433	33966	15.858		
Total	539533.711	33968			

We found significant differences ($p<0.05$) among the three models in predicting $T_{min.}$ The test statistics are shown in Table 2. We then carried out multiple pair wise comparison.

Table 3 Multiple pair wise comparison of the three models for predicting T_{min} under RCP4.5

					95% Confidence Interval	
I-Model	J-Model	Mean Difference (I-J)	Std. Error	Sig.	Lower Bound	Upper Bound
GFDL-ESM2M	MIROC5	.118	.054	.080	.00	.24
	MRI-CGCM3	.389*	.053	.000	.26	.51
MIROC5	GFDL-ESM2M	-.118	.054	.080	-.24	.01
	MRI-CGCM3	.271*	.052	.000	.15	.40
MRI-CGCM3	GFDL-ESM2M	-.389*	.053	.000	-.51	-.26
	MIROC5	-.271*	.052	.000	-.40	-.15

*. The mean difference is significant at the 0.05 level.

The statistics in Table 3 showed significant differences ($p<0.05$) between MRI-CGCM3 and GFDL-ESM2M models. The models MIROC5 and MRI-CGCM3 were also significantly different ($p<0.05$). However, no significant differences were observed between the MIROC5 and the GFDL-ESM2M model ($p>0.05$). Also see Figure 3.7 for pictorial differences. The MRI-CGCM3 model may be excluded in predicting minimum temperature under RCP4.5.

Table 4 Analysis of variance for predicting T_{max} under RCP4.5

	Sum of Squares	df	Mean Square	F	Sig.
Between Groups	6026.939	2	3013.470	235.897	.000
Within Groups	433899.301	33966	12.775		
Total	439926.240	33968			

There were significant differences ($p<0.05$) among the three models in predicting T_{max} under RCP4.5 as shown in Table 4.

Table 5 Multiple pair wise comparison of the three models for predicting T_{max} under RCP4.5

					95% Confidence Interval	
I-Model	J-Model	Mean Difference (I-J)	Std. Error	Sig.	Lower Bound	Upper Bound
BNU-ESM	CanESM2	-.682*	.048	.000	-.80	-.57

	MIROC-ESM-CHEM	-1.012*	.047	.000	-1.12	-.90
CanESM2	BNU-ESM	.682*	.048	.000	.57	.80
	MIROC-ESM-CHEM	-.330*	.047	.000	-.44	-.22
MIROC-ESM-CHEM	BNU-ESM	1.012*	.047	.000	.90	1.12
	CanESM2	.330*	.047	.000	.22	.44

*. The mean difference is significant at the 0.05 level.

Multiple pair wise comparison showed significant differences ($p<0.05$) between all of the three possible pairs as shown in Table 5. The amount of overlap in Figure 3.8 also supports this. If the models are to be used for making predictions, they have to be applied independently.

Table 6 Analysis of variance for predicting T_{min} and T_{max} under RCP8.5

		Sum of Squares	df	Mean Square	F	Sig.
T_{min}	Between Groups	1936.562	2	968.281	60.837	.000
	Within Groups	540600.027	33966	15.916		
	Total	542536.589	33968			
T_{max}	Between Groups	1543.572	2	771.786	61.179	.000
	Within Groups	428484.739	33966	12.615		
	Total	430028.311	33968			

Significant differences ($p<0.05$) were obtained among the three models in predicting both T_{min} and T_{max} under RCP8.5. The test statistics are shown in Table 6.

Table 7 Multiple pair wise comparison of the three models for predicting T_{min} and T_{max} under RCP8.5

Dependent Variable	I-Model	J-Model	Mean Difference (I-J)	Std. Error	Sig.	95% Confidence Interval	
						Lower Bound	Upper Bound
T_{min}	BNU-ESM	MIROC5	.482*	.054	.000	.35	.61
		MRI-CGCM3	.528*	.053	.000	.40	.65
	MIROC5	BNU-ESM	-.482*	.054	.000	-.61	-.35
		MRI-CGCM3	.046	.052	.764	-.08	.17
	MRI-CGCM3	BNU-ESM	-.528*	.053	.000	-.65	-.40
		MIROC5	-.046	.052	.764	-.17	.08
T_{max}	BNU-ESM	MIROC5	.456*	.048	.000	.34	.57
		MRI-CGCM3	.449*	.048	.000	.34	.56
	MIROC5	BNU-ESM	-.456*	.048	.000	-.57	-.34
		MRI-CGCM3	-.007	.046	.998	-.12	.10
	MRI-CGCM3	BNU-ESM	-.449*	.048	.000	-.56	-.34
		MIROC5	.007	.046	.998	-.10	.12

*. The mean difference is significant at the 0.05 level.

Multiple pair wise comparison showed that there were significant differences ($p<0.05$) in the prediction of T_{min} by the BNU-ESM and MIROC5 models as shown in Table 7. Similar results were obtained for the BNU-ESM and MRI-CGCM3 models. However, no significant differences ($p>0.05$) were observed between the MIROC5 and the MRI-CGCM3 models. This is in agreement with the results shown in Figure 3.9. The same trend was observed in the prediction of T_{max} by the three models as shown in Table 7 (also see Figure

3.10). The BNU-ESM model may be excluded in predicting both T_{min} and T_{max} under RCP8.5.

Table 8 Analysis of variance for predicting *R* under RCP4.5

	Sum of Squares	df	Mean Square	F	Sig.
Between Groups	401.948	2	200.974	3.087	.051
Within Groups	2211533.046	33966	65.110		
Total	2211934.994	33968			

The three models were not significantly different (p>0.05) in predicting rainfall under RCP4.5. The three models GFDL-ESM2G, MRI-CGCM3 and GFDL-ESM2M may be used concurrently.

Table 9 Analysis of variance for predicting *R* under RCP8.5

	Sum of Squares	df	Mean Square	F	Sig.
Between Groups	764.560	2	382.280	6.261	.002
Within Groups	2073592.791	33964	61.053		
Total	2074357.351	33966			

The three models were significantly different (p<0.05) in predicting rainfall under RCP8.5.

Table 10 Multiple pair wise comparison of the three models for predicting *R* under RCP8.5

					95% Confidence Interval	
I-Model	J-Model	Mean Difference (I-J)	Std. Error	Sig.	Lower Bound	Upper Bound
GFDL-ESM2G	GFDL-ESM2M	.18910	.10616	.206	-.0622	.4405
	MRI-CGCM3	.36745*	.10403	.000	.1213	.6136
GFDL-ESM2M	GFDL-ESM2G	-.18910	.10616	.206	-.4405	.0622
	MRI-CGCM3	.17834	.10130	.215	-.0615	.4182
MRI-CGCM3	GFDL-ESM2G	-.36745*	.10403	.000	-.6136	-.1213
	GFDL-ESM2M	-.17834	.10130	.215	-.4182	.0615

*. The mean difference is significant at the 0.05 level.

Multiple pair wise comparison indicated significant differences (p<0.05) between the GFDL-ESM2G and MRI-CGCM3 models under the RCP8.5. The GFDL-ESM2G and GFDL-ESM2M models were not significantly different (p>0.05). Similarly, the GFDL-ESM2M and the MRI-CGCM3 models were not significantly different (p>0.05) in predicting rainfall under RCP8.5. Linking statistical results and PDFs in Figure 3.12, the GFDL-ESM2G model predicts higher values of rainfall; MRI-CGCM3 predicts low values of rainfall while GFDL-ESM2M predicts moderate values. We recommend the use of the three models to allow for comparison of predictions. Table 11 is a summary of the selected models under different RCPs.

Table 11 Summary of selected models

Climatic variable	Selected models	Comment
RCP4.5		
Minimum temperature	MIROC5 and GFDL-ESM2M	MRI-CGCM3 excluded
Maximum temperature	BNU-ESM, CanESM2 and MIROC-ESM-CHEM	All models predicted differently
Rainfall	GFDL-ESM2G, MRI-CGCM3 and GFDL-ESM2M	No significant differences
RCP8.5		
Minimum temperature	MIROC5 and MRI-CGCM3	BNU-ESM excluded
Maximum temperature	MIROC5 and MRI-CGCM3	BNU-ESM excluded
Rainfall	GFDL-ESM2G, GFDL-ESM2M and MRI-CGCM3	High, moderate and low predictors respectively

IV. Conclusions

Climate projections of the mid-century were analysed using a subset of global climate models from the Coupled Model Inter-comparison Project 5. The projections were based on moderate and high climate change scenarios. All the three models used projected a rise in temperature by about 1 °C in the period 2040-2070 relative to the 1980-2010 reference period. However, in some cases, some models were excluded because they predicted differently. The three models used to simulate rainfall change were found to be consistent in simulating extremes. We therefore recommend that such models be used by sectors that are vulnerable to extreme rainfall such as drought and floods.

References

[1] Boberg, F., Berg, P., Thejll, P., Gutowski, W. J. and Christensen, J. H. 2009. Improved confidence in climate change projections of precipitation further evaluated using daily statistics from ENSEMBLES models. Climate Dynamics 35:1509-1520. doi 10.1007/s00382-009-0683-8.

[2] Carmen Sa´nchez de Cos, C., Sa´nchez-Laulhe´, J.M., Jime´nez-Alonso, C., Sancho-Avila, J.M. and Rodriguez-Camino, E. 2013. Physically based evaluation of climate models over the Iberian Peninsula. Climate Dynamics 40:1969-1984 DOI 10.1007/s00382-012-1619-2.

[3] Chiew, F.H.S., Kirono, D.G.C., Kent, D. and Vaze, J. 2009. Assessment of rainfall simulations from global climate models and implications for climate change impact on runoff studies. 18th World IMACS / MODSIM Congress, Cairns, Australia. http://mssanz.org.au/modsim09. (Last accessed 26/06/2013).

[4] Houghton, J. T., Ding, Y., Griggs, D. J., Noger, M., van der Linden, P. J., Dai, X., Maskell, K. and Johnson, C. A. Eds. 2001. Climate Change 2001: The Scientific Basis. Cambridge University Press, 881 pp.

[5] Johnson, F. and Sharma, A. 2009. Measurement of GCM Skill in Predicting Variables Relevant for Hydroclimatological Assessments. Journal of Climate 22: 4373-4382.

[6] Masanganise, J., Magodora, M., Mapuwei, T. and Basira, K. 2014a. An assessment of CMIP5 global climate model performance using probability density functions and a match metric method. Science Insights: An International Journal 4(1): 1-8.

[7] Masanganise, J., Mapuwei, T.W., Magodora, M. and Basira, K. 2014b. Multi-Model Projections of Temperature and Rainfall under Representative Concentration Pathways in Zimbabwe. International Journal of Science and Technology 3(4): 229-240.

[8] Masanganise, J., Chipindu, B., Mhizha, T., Mashonjowa, E. and Basira, K. 2013. An evaluation of the performances of Global Climate

[9] Models (GCMs) for predicting temperature and rainfall in Zimbabwe. International Journal of Scientific and Research Publications 3:1-11.

[10] Perkins, S. E., Pitman, A. J., Holbrook, N. J. and Mcaneney, J. 2007. Evaluation of the AR4 Climate Models' Simulated Daily Maximum

[11] Temperature, Minimum Temperature, and Precipitation over Australia Using Probability Density Functions. Journal of Climate 20: 4356-4376.

[12] Pitman, A. J. and Perkins, S. E. 2008. Regional Projections of Future Seasonal and Annual Changes in Rainfall and Temperature over

[13] Australia Based on Skill-Selected AR4 Models. Earth Interactions 12: 1-50. doi: http://dx.doi.org/10.1175/2008EI260.1.

[14] Randall, D. A. and Co-authors. 2007. Climate models and their evaluation. Climate Change 2007: The Physical Science Basis, S. Solomon et al., Eds., Cambridge University Press, 589-662.

Authors

First Author – J. Masanganise, Department of Physics and Mathematics, Bindura University of Science Education, P Bag 1020, Bindura, Zimbabwe, E-mail: jn.masanganise@gmail.com
Second Author – T.W. Mapuwei, Department of Physics and Mathematics, Bindura University of Science Education, P Bag 1020, Bindura, Zimbabwe
Third Author – M. Magodora, Department of Physics and Mathematics, Bindura University of Science Education, P Bag 1020, Bindura, Zimbabwe
Fourth Author – C. Shonhiwa, Department of Physics and Mathematics, Bindura University of Science Education, P Bag 1020, Bindura, Zimbabwe